

Flexural behavior of retrofitted RC columns by FRP-MF, Experimental approach

Navideh Mahdavi*¹ and Abbas Ali Tasnimi^{2a}

¹ Department of Civil Engineering, Faculty of Engineering, Marand Branch, Islamic Azad University, Marand, Iran

² Department of Structural Engineering, Faculty of Civil and Environmental Engineering, Tarbiat Modares University, Tehran, Iran

(Received October 28, 2018, Revised March 17, 2019, Accepted October 16, 2019)

Abstract. Most of the recent studies have improved the efficiency of FRP jackets for increasing the compressive strength, shear strength, and ductility of reinforced concrete columns; however, the influence of FRP jackets on the flexural capacity is slight. Although new methods such as NSM (near surface mounted) are utilized to solve this problem, yet practical difficulties, behavior dependency on adhesives, and brittle failure necessitate finding better methods. This paper presents the results of an experimental study on the application of fiber-reinforced polymer fastened mechanically to the concrete columns to improve the flexural capacity of RC columns. For this purpose, mechanical fasteners were used to achieve the composite behavior of FRP and concrete columns. The experimental program included five reinforced concrete columns retrofitted by different methods using FRP subjected to constant axial compression and lateral cyclic loading. The experimental results showed that the use of the new method proposed in this paper increased the flexural strength and lateral load capacity of the columns significantly, and good composite action of FRP and RC column was achieved. Moreover, the experimental results were compared with the results obtained from the analytical study based on strain compatibility, and good proximity was reached.

Keywords: FRP; RC columns; mechanical fasteners; flexural strengthening

1. Introduction

There is an essential need for strengthening of concrete structures for many reasons including increased loads, design or construction errors, change of functionality, and so on. Different methods have been developed over the years for solving different rehabilitation problems. In recent years, fiber-reinforced polymer (FRP) as a substantial material used widely for strengthening and retrofitting of reinforced concrete structures. The mechanical properties such as high strength to weight ratio, corrosion resistance, high resistance against fatigue failure, high damping, low thermal coefficient and the ease in application, are some advantages of FRP (Wu *et al.* 2007). Based on the design objectives, using FRP laminates and sheets may cause improvements in structural performance such as load-deformation capacity, stiffness, durability, and service ability. Despite promising development in the implementation of FRP for the repair and retrofit of reinforced concrete columns, only a few research investigations are available to deal with the flexural retrofitting of RC columns using FRP sheets or laminates.

RC elements generally fail by either crushing of concrete in compression and/or yielding of internal steel reinforcement. Although FRPs laminates have high strength,

they are brittle. These materials are designed and loaded in tension and they show linear elastic stress–strain behavior which is followed by a brittle failure without a yielding plateau. In the flexural strengthening of columns, FRP sheets are bonded to the side surfaces of columns. If the bond between concrete and adhesive remains intact, stresses can be transferred from concrete to FRP, and vice versa and full composite action will occur. On the other hand, when premature de-bonding occurs, the composite action is lost, and the strengthened column cannot reach the theoretical ultimate capacity. If an FRP-strengthened column retains its composite action, there are a possible failure of concrete crushing prior to, or after, tensile yielding of reinforcement. In most of these studies, RC columns have been retrofitted using FRP jackets, and because of the lateral confinement to the concrete, improvement of compression strength, shear strength, and ductility were reported (Saadatmanesh *et al.* 1994). However, improvement of flexural capacity in most of the cases was insufficient (Promis and Ferrier 2012). Moreover, one of the most important challenges in using FRP for the rehabilitation of concrete members is the brittle behavior of RC members strengthened with FRP due to rupture or debonding of FRP (Lezgy-Nazargah *et al.* 2018). In addition, the effect of the linear behavior of FRP materials makes the failure mechanism of FRP-strengthened RC members more complicated. In recent researches, the use of mechanical fasteners (MF) is emerging as a solution to improve the structural behavior of FRP-strengthened members (Lamanna 2002, Nardone *et al.* 2011, Jawdhari and Fam 2018, Atea 2017). The MF-FRP systems consist of pre-cured FRP sheets or laminates connected to the concrete

*Corresponding author, Ph.D., Assistant Professor,

E-mail: Nvdh_Mahdavi@Marandiau.ac.ir

^a Professor

surface by means of steel nails, anchor bolts, concrete screws or combination thereof.

In general, the primary role of FRP anchorage is to prevent or delay the process of debonding. However, in some cases, they are used to change the sudden brittle failure to ductile failure mode and provide load transfer mechanism at the critical sections (Jumaat and Alam 2010, Ekenel *et al.* 2006, Martin and Lamanna 2008, Bank and Arora 2007, Rizzo *et al.* 2005, Napoli *et al.* 2010, Bischof *et al.* 2014, Behera *et al.* 2016). In this paper, a new MF-FRP system is proposed and has been experimentally demonstrated aiming to improve the flexural capacity of RC columns subjected to bending and axial load. The results showed that this method could change the failure mechanism and improve the overall seismic behavior of FRP-strengthened RC columns.

2. Experimental program

The experimental program is made of flexural tests carried out on five RC column specimens at the structural engineering laboratory of International Institute of

Earthquake Engineering and Seismology (IIEES).

2.1 Specimens

Five column specimens of an approximately 1/3 scale were designed according to ACI 318-2014 and Iranian standard 2800. Geometry and detailing of all column specimens are shown in Fig. 1.

Four longitudinal bars of 14 mm diameter, with the volumetric ratio of 1.53% are the main reinforcement. Steel stirrups with a diameter of 10 mm were used as transverse reinforcement at the spacing of 50 mm for 160 mm top and bottom of columns height and at 100 mm for the remaining portion as depicted in Fig. 1. The foundation and cap beam was designed to apply the boundary condition and loads. Each tested specimens were designated according to their characteristics listed in Table 1.

2.2 Material properties

A normal-strength concrete mix-design carried out according to ACI 211.1 using type-II Portland cement. The mixing proportions of 1.0:1.6:2.3 (cement, fine, and coarse

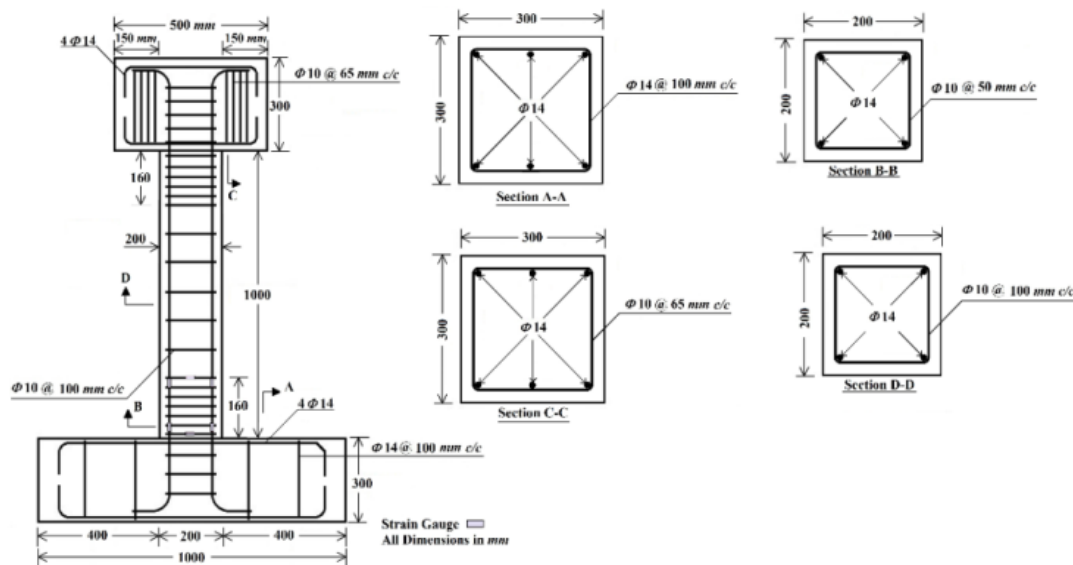


Fig. 1 Geometry and detailing of all RC column specimens

Table 1 Characteristics of the five tested specimens

Specimen denominations	Specimen description
RCO	Un-strengthened column to serve as the reference specimen.
SC1	Strengthened column using longitudinal FRP layers, which were extended on the concrete foundation as much as the anchorage length of the FRP layers.
SC2	Strengthened column similar to SC1 but using FRP jackets in both the top and bottom of the column to confine the concrete in plastic hinge zones.
SC3	Strengthened column using the longitudinal FRP layers, and mechanical fasteners to fix the FRP layers to the foundation and the RC column.
SC4	Strengthened column using the longitudinal FRP layers, and mechanical fasteners and FRP jackets were used in plastic hinge zones.

Table 2 Properties of materials

Material	Properties	Application of materials
Concrete	$f_c = 22.51$ (MPa), $E_s = 22.81$ (GPa), $\rho = 0.002$	-
Steel bars- $\Phi 14$	$f_y = 411.6$ (MPa), $E_s = 182$ (GPa)	Longitudinal reinforcement
Steel stirrups- $\Phi 10$	$f_y = 322.4$ (MPa), $E_s = 142$ (GPa)	Transverse reinforcement
FRP Sheet	$F_{au} = 3800$ (MPa), $E_a = 240$ (GPa), $\varepsilon_{au} = 0.0155$	Flexural strengthening of RC specimens
Epoxy Resin	$F_{au} = 54$ (MPa), $E_a = 3$ (GPa), $\varepsilon_{au} = 0.025$	Flexural strengthening of RC specimens

aggregate) with 0.48 w/c ratio and maximum aggregate size of 12 mm were used for all specimens. Cast specimens were de-molded after 24 hours and cured for 28 days using wet blankets covered with plastic sheeting. From the six 150×300 mm concrete cylinders, three were tested in compression at 28 days and the remaining three used for the tensile splitting test. The modulus of elasticity of concrete was calculated on the basis of data obtained from cylinder compression tests. The concrete strain corresponding to its strength was measured for each specimen. Longitudinal and transverse reinforcement comprised deformed steel bars of 14 and 10 mm diameters respectively. Only one type of FRP (CFRP) was used for vertical and/or horizontal wraps in all schemes. It was imperative for the study that the materials used be of identical properties for all columns. Consequently, all specimens were cast simultaneously with ready mixed concrete with steel reinforcement obtained from the same batch. Table 2 summarizes the average values of three samples of all the material used.

The surface of all RC columns was prepared prior to the application of FRP wraps. The concrete surface was prepared using hand grinders to roughen the surface and create the desired texture. The dust removed by vacuuming

the surface and an even layer of epoxy was applied to the prepared concrete. Then resin-saturated sheets of FRP were placed on the prepared concrete surface.

Method of surface preparation in all the retrofitted columns, the same layer of longitudinal FRP was used on two opposite column sides before applying the transverse layer and/or mechanical fasteners. FRP layers were extended on the top face of concrete foundation as much as anchorage length. Fig. 2 shows the detail of the retrofitted columns.

For both SC2 and SC4 columns, the transverse layers of FRP were used to confine the concrete at the plastic hinge zones. Finally, mechanical fasteners (MFs) were used to fix the FRP layers to the RC column and especially the column-to-foundation connection. After the FRP was allowed to cure for about 24 hours, the anchorage system was assembled. First, two holes spaced 30 centimetres were drilled along the column, and two bolts were then placed into these holes and fixed with two nuts on both sides. In the column-to-foundation connection, an angle section was bolted to the foundation and the RC column. The angle with two stiffeners was designed and constructed for every side of the column. Three holes in the foundation and one hole in the column were drilled and filled with Hilti-RE500 Epoxy after the holes were sufficiently cleaned. The anchorage angles were placed into their final position while the epoxy was still wet. Then bolts were placed. Fig. 3 shows the detail of MF system used in the foundation connection.

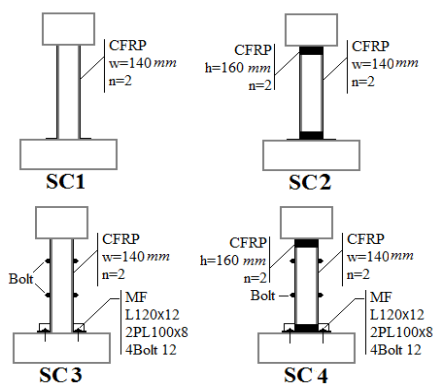
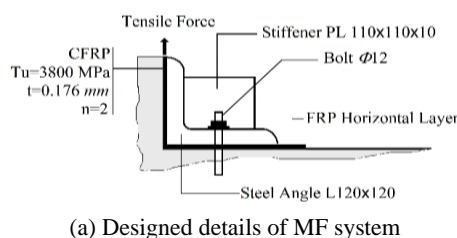


Fig. 2 FRP strengthening layouts, all specimens

2.4 Test loading and instrumentation

The test setup consisted of a reaction frame fixed to the strong floor and supporting the lateral and vertical hydraulic actuators. So, the retrofitted columns were tested under combined axial and lateral loads. The main components of the strong floor are the two transverse beams placed on the RC foundation and fixed to the floor by means of four high strength rods that were properly pre-tensioned in order to



(a) Designed details of MF system



(b) Mechanical fasteners used to retrofit columns

Fig. 3 Mechanical fastener designed in foundation connection

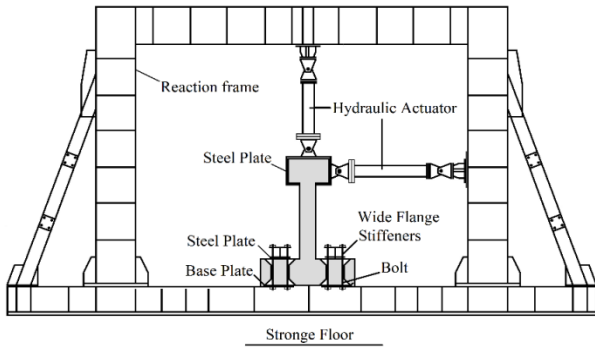


Fig. 4 Schematic test setup details

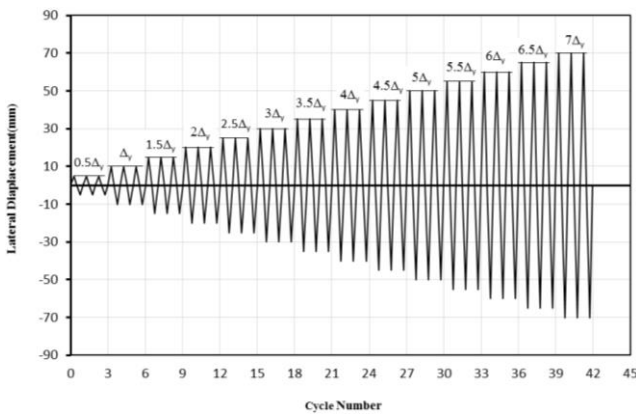


Fig. 5 Loading protocol

avoid any stub-rotation. Fig. 4 shows the test setup and details of the loading system.

Before application of the lateral load, the RC columns were first loaded with a constant axial load using a hydraulic jack at the top. The 200 kN axial load applied primarily was approximately 25% of the ultimate axial load capacity and this axial load was constant during the application of lateral load. After initial axial loading, the lateral load was applied using a hydraulic actuator in a displacement control mode. The applied displacement amplitude was a fraction of the estimated tip yield displacement. The amplitude of the lateral cyclic displacement was chosen in multiples of $0.5\Delta_y$, with three cycles applied to each amplitude of displacement. Fig. 5 shows the loading protocol applied to all the specimens.

Linear variable displacement transducers (LVDTs) were

used to record the horizontal displacements of the columns as well as any vertical movement of the footing. Eight strain gages per specimen were used to measure the developed strain in the longitudinal reinforcement at both sides of the RC column and the tensile strains in the CFRP strips as well.

3. Results and discussion

In the following, the most criteria related to the failure modes for un-strengthened RC columns and FRP-strengthened RC columns are discussed in detail. The considered criteria include the mode of failure, hysteresis curves, ultimate capacity, ultimate developed tensile strains, stiffness degradation, and energy dissipation.

3.1 Failure modes and crack patterns

All the relevant test results, including drift related to the first crack and FRP de-bonding, drift at yielding of the steel reinforcement (δ_y), maximum lateral load and drift at ultimate state (F_u , δ_u), ductility, percentage variation of lateral strength and lateral drift with respect to the control specimen are presented in Table 3. The values of δ_y are defined as the level at which the strain in the steel reinforcement reaches a measured value of $2000 \mu\epsilon$. The values of F_u and of the associated displacement δ_u are defined as the level at which the maximum load is reached (Fig. 6).

The failure mode and the crack pattern of all specimens are illustrated in the photographs of Fig. 7. The failure mode of all the tested specimens was controlled by flexure due to their high ratio of transverse reinforcement and a low ratio of longitudinal reinforcement. The control specimen,

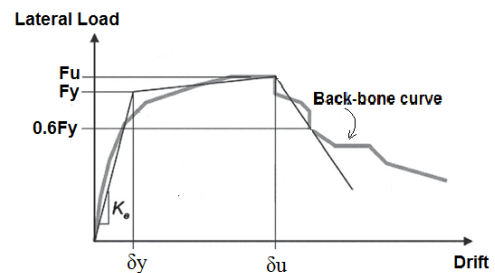


Fig. 6 Back-bone curve and idealized curve according to ASCE 41-13

Table 3 Experimental results and failure characteristics, all specimens

Column specimens	Drift at first crack (%)	Drift at first FRP de-bonding (%)	Ultimate load (kN)	Drift at ultimate load (%)	Drift at yielding (%)	Ultimate drift (%)	Increase in F_u (%)	Increase in δ_u (%)	Ductility
RCO	0.5	-	9.50	2.5	1.06	3.3	-	-	3.09
SC1	0.5	0.3	10.1	2.5	1.11	3.5	6.3	6.1	3.15
SC2	1.0	0.5	14.64	2.5	1.23	3.8	54	15	3.07
SC3	2.0	-	20.15	3.0	1.25	5.5	112	66	4.36
SC4	2.2	-	19.85	3.5	1.26	6.0	109	82	4.76

RCO, failed in flexure by yielding of the steel reinforcement, followed by crushing of the concrete in the plastic hinge zone as shown in Fig. 7.

The strengthened columns, in general, showed higher lateral drifts at cracking than the control column. Observations during the first test in column RCO indicated that the first crack was formed at the tension side at 0.5% drift ratio occurred at about 150 mm distance from the base of the column. As the lateral displacement reached the value of 2.5%, the specimen reached the maximum capacity of the lateral resistance strength. After that, the concrete cover experienced extensive cracking. Besides, the buckling of longitudinal bars happened with the crushing of the concrete.

In the SC1 and SC2 specimens, buckling of the longitudinal bars occurred after de-bonding of the FRP strips. As shown in Fig. 7, strengthened RC columns in this group could not develop composite action due to the de-bonding of the FRP strips. In both specimens during testing, a crackling noise revealed the progressive cracking of the epoxy paste, until the epoxy cover was split and de-bonding of the FRP strips occurred in the first cycles of lateral loading; then both FRP strips and RC column resisted lateral displacement individually. Therefore, SC1 exhibited a similar response to the RCO specimen in terms of post-yielding stiffness and strength with a slight increase in strength (6.3%), while a 54% strength increase was attained in SC2.

The fact that the failure was not governed by the composite behavior of FRP and reinforced concrete, as expected, emphasizes the sensitivity of EB-FRP systems to the adhesive bonding procedure. The first flexural cracking occurred when the specimen was subjected to a drift level of 0.5% in specimen SC1 and 1% in specimen SC2. The lateral resistance reached the maximum value at the displacement of about 2.5% for both specimens. Both of the MF-FRP strengthened RC columns showed similar failure

mechanism and failed by yielding the steel reinforcement followed by crushing the concrete and splitting the FRP strips. No apparent de-bonding was observed except some very weak sound of epoxy cracking. The first flexural cracking occurred when the specimens SC3 and SC4 experienced a drift level of 2% and 2.2% respectively. The lateral resistance reached the maximum value at the displacement of about 3% for SC3 and 3.5% for SC4. The ultimate strength for SC3 and SC4 increased by 112% and 109% percent respectively compared with the un-strengthened RCO column. Therefore, the failure modes of the MF-FRP-strengthened columns showed that using an appropriate anchorage system could transfer the stress between the concrete and the FRP reinforcement in order to develop composite action. The strengthening configuration adopted for SC4 column showed the best results, meaning that MFs changed the failure mechanism significantly. This, in turn, delayed the appearance of cracks, changed the sequence of failure and increased the ultimate capacity.

3.2 Hysteresis and envelop curves

Lateral load versus lateral displacement for all columns are shown in Fig. 8 in the form of hysteresis curves. The RCO and SC1 showed almost the same behavior until the failure due to the de-bonding of FRP strips occurs before the appearance of the first crack for SC1 and leads to negligible improvement in both load and displacement for this column. In the case of SC2 (the EB-FRP strengthened column), the load and displacement hysteresis curves develop to some extent, but the shape of the hysteresis loop and the rate of the strength decrease in post-yielding are the same. It is clear that although in the first loops, changing in the initial stiffness and lateral strength is obvious, after de-bonding of the FRP strips, the strengthening influences is dimming.

For the MF-strengthened RC column, SC3, the FRP was

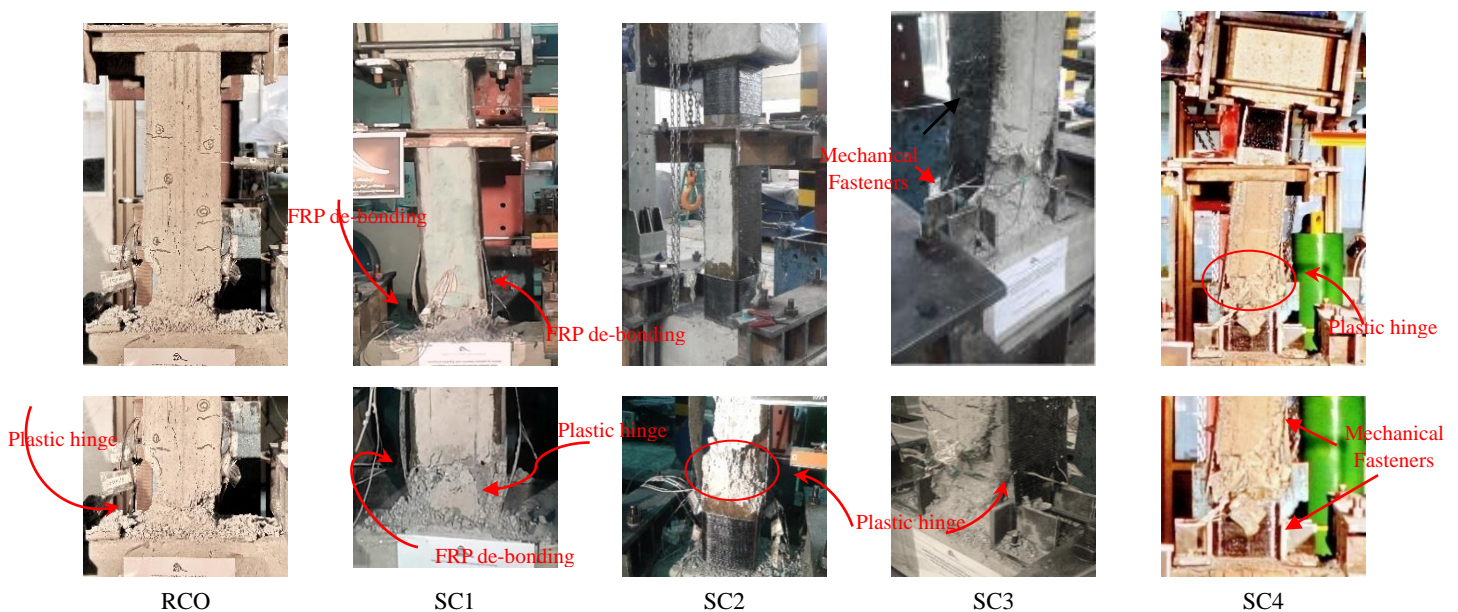
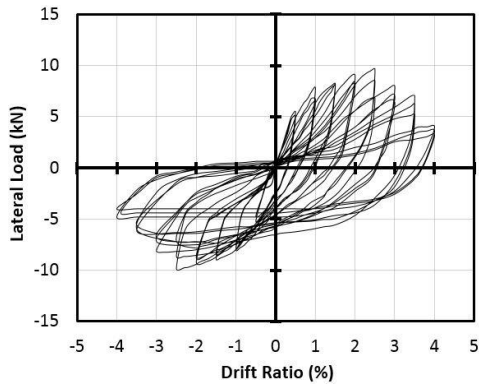
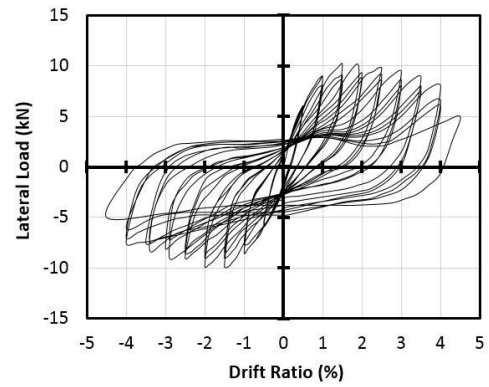


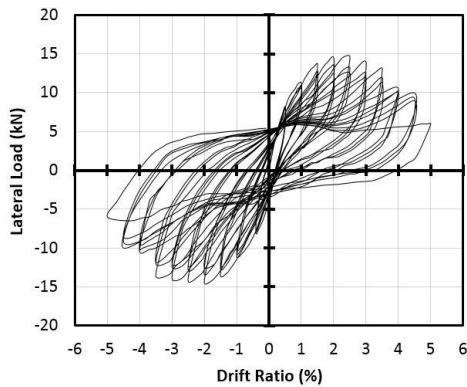
Fig. 7 Failure modes of all specimens



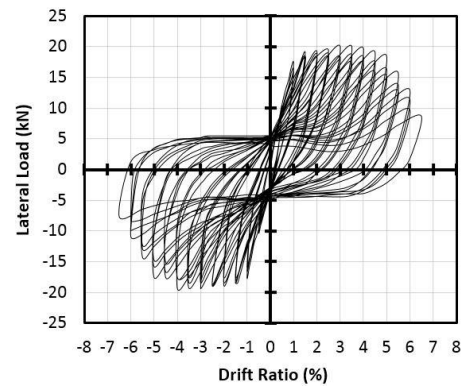
Un-strengthened RC column, Specimen RCO



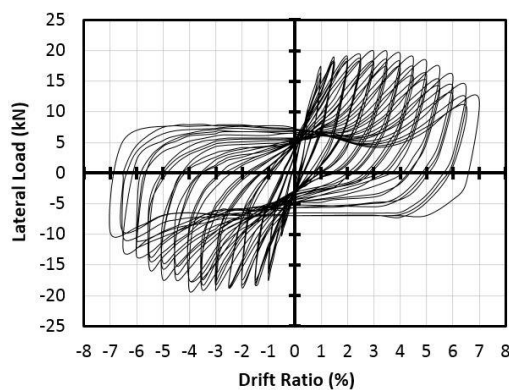
Strengthened using longl. FRP, Specimen SC1



Strengthened longl. FRP and FRP jackets, Specimen SC2



Strengthened using longl. FRP and MF, Specimen SC3



Strengthened using longl. FRP, FRP jackets and MF, Specimen SC4

Fig. 8 Hysteresis curves for all of the specimens

fastened by mechanical anchors improved the overall lateral strength as compared to the un-strengthened specimens. The even increase in lateral load and displacement shows a composite action between the FRP strips and the RC column. According to Fig. 8, the combination of FRP strips fastened mechanically and FRP jacketing in the plastic zones displays the best response characteristics, thereby making the strength to increase to approximately 19.85 kN.m in this specimen, which was nearly double that of the control specimen. Fig. 9 compares the envelopes of lateral load-displacement behavior of specimens. As can be seen, the measured drifts observed at the first cracking for the FRP-strengthened columns are higher than those of the un-

strengthening specimens. However, the drifts for the EB-FRP specimens related to the first crack are close to that of the un-strengthening specimen as the de-bonding mechanism develops. For MF-FRP specimens, SC3 and SC4, the delay in appearance of the first crack are obvious.

At yielding of the steel reinforcement, the columns strengthened with MF-FRP exhibited increasing the yield drift with respect to the control specimen ranging from 16% for SC2 to 18.8% for SC4. However, for C1 specimen, the increase was slight. (4%). At ultimate, the columns strengthened with MF-FRP exhibited increase nearly double that of the control specimen, and the lateral drift increased ranging from 66% to 82%.

Table 4 Maximum tension strain in ultimate lateral load

Column specimen	Max ϵ_t in FRP ($\mu\epsilon$)	Max ϵ_t in tension steel ($\mu\epsilon$)	Max ϵ_t in transverse steel ($\mu\epsilon$)
RCO	-	4138	521
SC1	614	3969	515
SC2	1443	3833	190
SC3	4815	3805	863
SC4	4771	3765	702

3.3 Ultimate tensile strains

Table 4 shows the average tension strain at ultimate lateral load in tension steel, transverse steel, and FRP strips. Measurement of strain in FRP strips at or near the column-foundation joint could be used to determine the force developed in the FRP which would allow for an evaluation of the force transfer mechanism in FRP strips and the new anchorage system.

According to Table 4, in strengthened columns compared with un-strengthened RCO column, yielding of reinforcement bar takes place, generally, later, and using longitudinal FRP reduces the strain values of tension bars. Contrary to what is generally expected, comparison of specimens SC1, SC2, and the un-strengthened RCO column show that the tension strains of FRP strips are much different at the ultimate lateral load. The apparent explanation is the de-bonding of FRP strips by increasing the imposed displacement though the difference in the tension strain values of specimens SC1 and SC2 highlights the single behavior of RC column and FRP strips. This implies that the epoxy resin layer used mainly characterized the behavior of the EB-FRP strengthened members.

As expected, the FRP and the tension steel strain of specimens SC3 and SC4 were approximately relative, highlighting the efficiency of using the MF systems and longitudinal FRP strips to improve the flexural capacity of RC columns.

3.4 Stiffness degradation

Based on the experimental results, the mean value of stiffness for the i^{th} cycle can be evaluated using Eq. (1) given by Mayes and Clough (1975).

$$K = \frac{|F_{max,i}^+| + |F_{max,i}^-|}{|\Delta_{max,i}^+| + |\Delta_{max,i}^-|} \quad (1)$$

The stiffness of each displacement cycle, K , is then normalized with respect to that of the first cycle, K_i , thus providing a measure of the stiffness degradation. The relationships between K/K_i and drift ratio are plotted in Fig. 10. As shown, the un-strengthened column, RCO, exhibited a greater rate of stiffness degradation than the strengthened specimens.

Moreover, Fig. 10 illustrates that under low displacement values, the curves relative to specimens SC1,

SC2 and RCO overlap each other though it seems that the stiffness degradation is practically independent of the presence of FRP externally bonded. Conversely, the improved behavior is evident for the columns SC3 and SC4; in this case, MF-FRP strengthened RC columns, MFs caused the FRP strips to be fully engaged in the composite action from early steps of lateral loading. This observation was attributed to the fact that MF-FRP strengthened RC columns had a composite behavior.

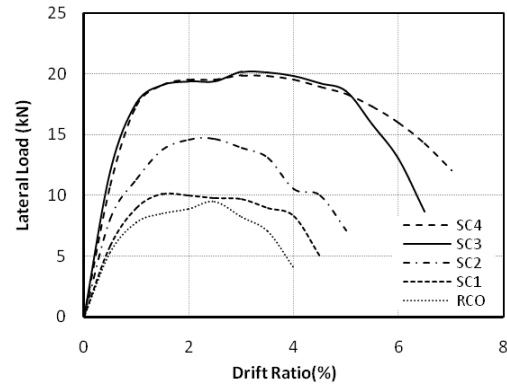


Fig. 9 Envelopes of the hysteresis curves of all specimens

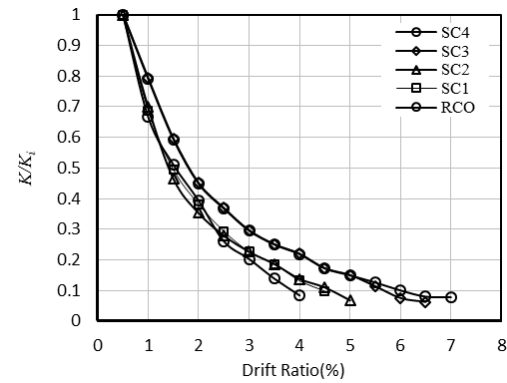


Fig. 10 Stiffness degradation for all specimens

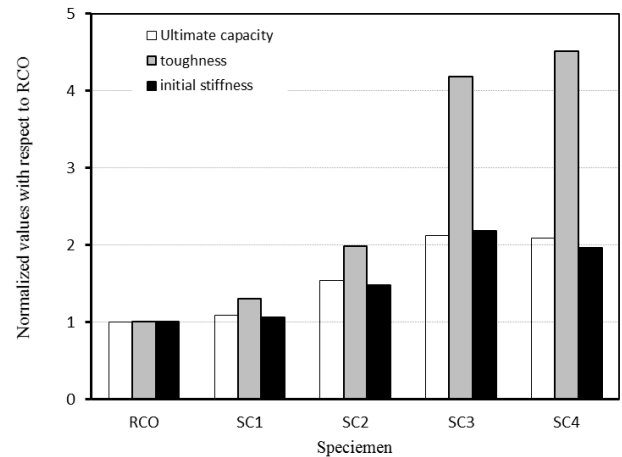


Fig. 11 Comparison among the normalized ultimate capacity, toughness and initial stiffness for all specimens

3.5 Initial stiffness, ductility, and energy dissipation

Ductility can be described as the ability of the structure or its components, or of the materials used to offer resistance in the inelastic domain of response. It includes the ability to sustain large deformations, and a capacity to absorb energy by a hysteretic behavior. Displacement ductility of a specimen was determined based on the ratio of ultimate displacement to yield displacement. The ultimate displacement defined as the displacement corresponding to a 20% strength degradation of the maximum strength of the specimen, and the yield displacement defined as displacement corresponding to the first yielding of the longitudinal column reinforcement. Table 3 shows the ductility values for all specimens.

A general observation was that using longitudinal FRP in conventional EB techniques could not improve the ductility of the specimens. As designated in Table 3, even with using the FRP jackets in plastic zones, the ductility of the FRP-strengthened column is lower than that of the un-strengthened one. This fact that using longitudinal FRP delays the yield displacement could be an appropriate description. Consequently, the longitudinal EB-FRP was not effective in improving the ductility of the FRP-strengthened RC columns.

On the other hand, in the presence of mechanical fasteners, the ductility of the columns significantly increased as shown in Table 3. 41% increase in SC3 and 54% increase in SC4 imply that using MF-FRP could improve the overall performance of RC columns since mechanical fastening is the means for the transfer of stress between the concrete and the FRP reinforcement in order to develop composite action. This can be attributed to the efficiency of the inclined MF-FRP strengthening technique in retrofitting the RC columns.

Another comparison criterion for RC columns is the initial stiffness. The initial stiffness is the slope of the first part of the load–displacement curve. Fig. 11 compares the specimens based on normalized initial stiffness. It can be seen that the FRP-strengthened column, SC1, has approximately the same value of the un-strengthened column. On the other hand, all of the strengthened columns showed higher values compared to specimens, RCO and SC1. In addition, the variations of the initial stiffness for the MF-FRP-strengthened columns were noticeable. Numerical results for the initial stiffness could be easily obtained from the load–displacement relationships for all the strengthened columns. As it is revealed in Figure 11, in the presence of MFs, the initial stiffness of the RC columns significantly increased; the increase of 2.18 times for the specimen SC3 and 1.96 times for SC4 conforms this assertion.

According to Mohy (Afefy *et al.* 2013), the toughness of a system is defined as the area under the load–displacement curve. It is used here as an indicator of energy dissipation. Higher toughness means higher dissipation of energy until the failure occurs.

Fig. 11 shows the comparison of columns from the normalized toughness viewpoint. From the toughness values, it can be concluded that all the FRP-strengthened

columns exhibited higher toughness except column SC1 that showed approximately the same toughness of column RCO. Also, the higher toughness estimated for SC3 and SC4 specimens could be attributed to the proper seismic behavior of RC columns strengthened using FRP and newly MF designed. Toughness increase of 4.18 times for SC3 and 4.51 times for SC4 was estimated. The results of accumulated energy dissipation clearly demonstrated that the retrofitted specimens using the FRP fastened mechanically to the RC columns dissipated more energy than the control specimen and the EB FRP-strengthened columns.

4. Analytical investigation

The analytical solution used for estimation of the flexural capacity of RC columns externally strengthened with MF-FRP is based on general strain compatibility and the internal forces equilibrium. The following assumptions were made in calculating the flexural resistance of a column section strengthened with an externally applied FRP and MF system:

- There is no relative slip between the external FRP and the concrete with using MF system.
- Mander 1988, stress-strain laws considered in the numerical analyses to simulate the behavior of concrete in compression. strain compatibility used to predict general compression strain of concrete.
- The shear deformation within the adhesive layer is neglected since it is very thin.
- FRP layers have a linear elastic stress-strain relationship to failure.
- The tensile strength of concrete was neglected.

The moment of resistance of the section about the neutral axis is given by

$$M_R = M_{st} + M_{sc} + M_{ct} + M_{CS} + M_{ft} \quad (2)$$

$$M_{st} = \sum_{k=1}^n A_{sk} f_{sk} (d_k - d_{ni}) \quad (3)$$

Moment due to tensile reinforcement is: (Tasnimi 2000)

where, A_{sk} and f_{sk} are the area and tensile stress of reinforcement in the tension side at the k^{th} level. d_{ni} is the depth of natural axis at the i^{th} state of loading. Moment due to compression reinforcement is

$$M_{sc} = \sum_{j=1}^n A_{sj} f_{sj} (d_{ni} - d'_k) \quad (4)$$

where, A_{sj} and f_{sj} are the area and stress of reinforcement in compression side at the j^{th} level. Moment due to concrete tensile strength is given by

$$M_{ct} = \frac{bd_{ni}^2}{3\varepsilon_{ci}^2} E_c \varepsilon_{ct}^3 \quad (5)$$

where, b is the section's width and ϵ_{ci} and ϵ_{ct} are the concrete's compressive strain and the concrete cracking strain, respectively. Moment due to concrete compression strength is

$$M_{cc} = \frac{bd_{ni}(d_{ni} - d_c)}{\epsilon_{ci}} \int_0^{\epsilon_{ci}} \sigma_{xi}(\epsilon_{xi})d\epsilon_{xi} \quad (6)$$

$$d_c = d_{ni} \left[1 - \frac{\int_0^{\epsilon_{ci}} \epsilon_{xi} \sigma_{xi}(\epsilon_{xi})d\epsilon_{xi}}{\epsilon_{ci} \int_0^{\epsilon_{ci}} \sigma_{xi}(\epsilon_{xi})d\epsilon_{xi}} \right] \quad (7)$$

where, σ_{xi} is the concrete compressive strain and ϵ_{xi} is the concrete strain at depth equal to $(d_{ni}-x_i)$. the parameter d_c obtained by

$$M_{ft} = A_{fk}f_{fk}(d_f - d_{ni}) \quad (8)$$

and moment due to FRP tensile force is

$$C_i = \frac{bd_{ni}}{\epsilon_{ci}} \int_0^{\epsilon_{ci}} \sigma_{xi}(\epsilon_{xi})d\epsilon_{xi} + \sum_{j=1}^n A_{sj}f_{sj} \quad (9)$$

where, A_{fk} and f_{fk} are the area and tensile stress of FRP in the tension side respectively. Also, the total compressive and tensile force of retrofitted section would be

$$T_i = 1/2bd_{ni} \frac{E_c \epsilon_{ct}^2}{\epsilon_{ci}} + \sum_{j=1}^m A_{sk}f_{sk} + A_{fk}f_{fk} \quad (10)$$

4.1 Analytical results

A computer program was coded and sectional geometry, mechanical properties of concrete, steel, and FRP were used

as the input data to predict the behavior of RC columns strengthened with MF-FRP systems. For simulating the behavior of steel rebar, concrete and FRP strips stress-strain (σ - ϵ) obtained relationships from experimental tests were used. The analytical and experimental results in every first cycle of the successive loading cycles are given in Table 5. According to this table, the analytical resistance moment gives reasonable predictions for the flexural capacity of RC columns strengthened with MF-FRP. However, unacceptable errors in the last cycles occur after the plastic hinge development. The results show the deficiencies in analytical solutions to estimate the flexural capacity of RC columns after rebar buckling and concrete crushing in the last cycles.

5. Conclusions

An experimental study has been presented aiming at better understanding the effect of MF-FRP strengthening systems on the flexural response of RC columns as an alternative new method for NSM (Near Surface Mounted) and other EB-FRP systems.

Five RC column specimens were tested to failure: a specimen which is the benchmark un-strengthened RC column (RC0), a similar specimen strengthened using longitudinal FRP layers (SC1); the other specimen was similar to SC1 but using FRP jackets at plastic hinge zones (SC2), C3 was strengthened using longitudinal FRP layers and MFs, and SC4 as strengthened similar to SC3 using FRP jackets at plastic hinge zones. From the experimental study, the following conclusions are drawn.

- (1) An increase in the ultimate lateral load of the MF FRP-strengthened RC columns was measured as 99.5% comparable with the un-strengthened and 37.6% comparable with the EB-FRP strengthened

Table 5 Experimental and analytical results for specimens SC3 and SC4

Cycle No.	Results for specimen SC3			Results for specimen SC4		
	Moment of resistance (kN-m)	Applied moment (kN-m)	Error (%)	Moment of resistance (kN-m)	Applied moment (kN-m)	Error (%)
1	12.58	11.53	9.1	11.71	11.48	2.03
2	19.43	20.24	4.0	18.73	19.96	6.16
3	21.28	21.94	3.0	20.50	21.96	6.64
4	22.43	22.26	0.7	20.90	22.46	6.96
5	22.87	22.26	2.7	22.05	22.46	1.82
6	23.09	23.17	0.3	22.05	22.73	3.01
7	24.12	23.14	4.2	22.05	22.82	3.37
8	23.81	22.79	4.5	21.85	22.47	2.74
9	23.50	22.08	6.4	22.80	21.76	4.79
10	21.85	21.34	2.4	22.41	21.06	6.38
11	17.92	18.17	1.4	20.20	19.91	1.45
12	16.91	14.93	13.3	19.35	18.42	5.06
13	13.04	9.98	30.6	17.85	16.40	8.84
14	-	-	-	17.68	13.86	27.49

- RC columns using FRP jackets at both ends.
- (2) An increase in the lateral displacement up to 82% was also observed in SC4, (MF FRP-strengthened RC column) comparable with the benchmark un-strengthened RC column and 57.9-71.4% comparing to the EB-FRP strengthened RC columns.
 - (3) Using the FRP jacketing in the MF-FRP strengthened specimen, increased the ductility of the column without any difference in the ultimate lateral load.
 - (4) The tensile strain in FRP in SC3 and SC4 specimens strengthened with MF-FRP was fairly relative to the tensile strain of steel bars which is indicative of an even load transfer.
 - (5) The sectional analysis showed good agreement with the experimental results in restoration of the analytical resistance moment and applied incremental moment for the MF-FRP strengthened RC columns.

Acknowledgments

The research described in this paper was financially supported by International Institute of Earthquake Engineering and Seismology (IIEES).

References

- ACI 211.1-91 (1991), Standard practice for selecting proportion for normal, heavy weight and mass concrete, American Concrete Institute.
- ACI 318-14 (2014), Building code requirements for structural concrete, commentary on building code requirements for structural concretes, American Concrete Institute.
- ACI 440.2R-02 (2005), Guide for the design and construction of externally bonded FRP systems for strengthening concrete structures, Reported by ACI Committee 440.
- Afey, H.M.E.D., Mahmoud, M.H. and Fawzy, T.M. (2013), "Rehabilitation of defected RC stepped beams using CFRP", *Eng. Struct.*, **49**, 295-305. <https://doi.org/10.1016/j.engstruct.2012.11.013>
- Atea, R.S. (2017), "Torsional behavior of reinforced concrete T-beams strengthened with CFRP strips", *Case Studies Constr. Mater.*, **7**, 110-117. <https://doi.org/10.1016/j.cscm.2017.03.002>
- Bank, L.C. and Arora, D. (2007), "Analysis of RC beams strengthened with mechanically fastened FRP (MF-FRP) strips", *J. Compos. Struct.*, **79**(2), 180-191. <https://doi.org/10.1016/j.compstruct.2005.12.001>
- Behera, G.C., Rao, T.G. and Rao, C.B.K. (2016), "Torsional behavior of reinforced concrete beams with ferrocement U-jacketing—experimental study", *Case Studies Constr. Mater.*, **4**, 15-31. <https://doi.org/10.1016/j.cscm.2015.10.003>
- Bischof, P., Suter, R., Chatzi, E. and Lestuzzi, P. (2014), "On the use of CFRP sheets for the seismic retrofitting of masonry walls and the influence of mechanical anchorage", *Polymers*, **6**(7), 1972-1998. <https://doi.org/10.3390/polym6071972>
- Ekenel, M., Rizzo, A., Myers, J.J. and Nanni, A. (2006), "Flexural fatigue behavior of reinforced concrete beams strengthened with FRP fabric and precured laminate systems", *J. Compos. Constr.*, **10**(5), 433-442. [https://doi.org/10.1061/\(ASCE\)1090-0268\(2006\)10:5\(433\)](https://doi.org/10.1061/(ASCE)1090-0268(2006)10:5(433))
- Jawdhari, A. and Fam, A. (2018), "Numerical study on mechanical and adhesive splices for ribbed GFRP plates used in concrete beams", *Eng. Struct.*, **174**, 478-494. <https://doi.org/10.1016/j.engstruct.2018.07.085>
- Jumaat, M.Z. and Alam, M.A. (2010), "Experimental and numerical analysis of end anchored steel plate and CFRP laminate flexural strengthened reinforced concrete (r. c.) beams", *Int. J. Phys. Sci.*, **5**, 132-144.
- Lezgy-Nazargah, M., Dezhangah, M. and Sepehrinia, M. (2018), "The effects of different FRP/concrete bond-slip laws on the 3D nonlinear FE modeling of retrofitted RC beams — A sensitivity analysis", *Steel Compos. Struct., Int. J.*, **26**(3), 347-360. <https://doi.org/10.12989/scs.2018.26.3.347>
- Lamanna, A.J. (2002), "Flexural strengthening of reinforced concrete beams with mechanically fastened fiber reinforced polymer strips", Ph.D. Thesis; University of Wisconsin-Madison, Madison, WI, USA.
- Mander, J.B., Priestley, M.J. and Park, R. (1988), "Theoretical stress-strain model for confined concrete", *J. Struct. Eng.*, **114**, 1804-1826. [https://doi.org/10.1061/\(ASCE\)0733-9445\(1988\)114:8\(1804\)](https://doi.org/10.1061/(ASCE)0733-9445(1988)114:8(1804))
- Martin, J.A. and Lamanna, A.J. (2008), "Performance of mechanically fastened FRP strengthened concrete beams in flexure", *J. Compos. Constr.*, **12**(3), 257-265. [https://doi.org/10.1061/\(ASCE\)1090-0268\(2008\)12:3\(257\)](https://doi.org/10.1061/(ASCE)1090-0268(2008)12:3(257))
- Mayes, R.L. and Clough, R.W. (1975), "State of the art in seismic shear strength of masonry — An evaluation and review", EERC Report; Berkeley, CA, USA.
- Napoli, A., Matta, F., Martinelli, E., Nanni, A. and Realfonzo, R. (2010), "Modeling and verification of response of RC slabs strengthened in flexure with mechanically fastened FRP laminates", *Magaz. Concrete Res.*, **62**(8), 593-605. <https://doi.org/10.1680/macr.2010.62.8.593>
- Nardone, F., Lignola, G.P., Prota, A., Manfredi, G. and Nanni, A. (2011), "Modeling of flexural behavior of RC beams strengthened with mechanically fastened FRP strips", *Compos. Struct.*, **93**(8), 1973-1985. <https://doi.org/10.1016/j.compstruct.2011.03.003>
- Promis, G. and Ferrier, E. (2012), "Performance indices to assess the efficiency of external FRP retrofitting of reinforced concrete short columns for seismic strengthening", *Constr. Build. Mater.*, **26**(1), 32-40. <https://doi.org/10.1016/j.conbuildmat.2011.04.067>
- Rizzo, A., Galati, N., Nanni, A. and Bank, L.C. (2005), "Strengthening concrete structures with mechanically fastened pultruded strips", *COMPOSITES 2005 Convention and Trade Show American Composites Manufacturers Association*, Columbus, OH, USA, September.
- Saadatmanesh, H., Ehsani, M.R. and Li, M.W. (1994), "Strength and ductility of concrete columns externally reinforced with fiber composite straps", *Struct. J.*, **91**(4), 434-447.
- Standard No. 2800 (2015), Iranian code of practice for seismic resistant design of buildings, ministry of housing and urban development of Iran, (4rd Edition), Tehran, Iran.
- Tasnimi, A.A. (2000), "Strength and deformation of mid-rise shear walls under load reversal", *J. Eng. Struct.*, **22**(4), 311-322. [https://doi.org/10.1016/S0141-0296\(98\)00110-2](https://doi.org/10.1016/S0141-0296(98)00110-2)
- Wu, Z.S., Wang, X. and Iwashita, K. (2007), "State-of-the-art of advanced FRP applications in civil infrastructure in Japan", *Compos. Polym.*, **37**, 1-17.